RSC Advances

ROYAL SOCIETY OF CHEMISTRY

www.rsc.org/advances

A Theoretical Study of Dirhodium-Catalyzed Intramolecular Aliphatic C−H Bond Amination of Aryl Azides†

Huiying Xu, Xuepeng Zhang, Zhuofeng Ke* and Cunyuan Zhao*

School of Chemistry and Chemical Engineering, Sun Yat-sen University, Guangzhou 510275, P. R. China. E-mail: kezhf3@mail.sysu.edu.cn; ceszhcy@mail.sysu.edu.cn; Fax: +8620 8411 0523; Tel: +8620 8411 0523

† Electronic supplementary information (ESI) available: The Cartesian coordinates for the calculated stationary structures.

ABSTRACT: Dirhodium-contained catalysts mediated aliphatic C−H bond amination of aryl azides were studied using BPW91 functional. Calculations show the reactions with $Rh_2(esp)_2$ (esp=α,α,α′,α′-tetramethyl-1,3-benzenedipropionic acid) and the model compound $Rh_2(OCHO)_4$ as catalysts take place via similar mechanisms. Firstly, the dirhodium metal complex coordinates with the substrate and releases nitrogen gas. This rate-determining step results in the formation of the metal nitrene. Metal nitrene mediated intramolecular C−H bond amination is conducted via two alternative pathways, respectively. The singlet metal nitrene mediated intramolecular C−H bond amination occurs via a concerted and asynchronous pathway involving direct metal nitrene insertion into the C−H bond. The triplet metal nitrene case is a stepwise pathway involving a hydrogen transfer and then a diradical recombination. Our study suggests the triplet H-abstraction is more favorable than the singlet one. The resulted triplet intermediate would not go through the high-barrier diradical recombination process, but across to the singlet pathway via a MECP and form the final singlet product. The tethered esp ligands in $Rh_2(esp)_2$ provide steric effects to constrain the substrate-catalyst compound but indicates inconspicuous influence on the mechanisms of dirhodium catalyzed aliphatic C−H bond amination of aryl azides.

1. Introduction

C−H functionalization is an efficient approach to obtain natural or unnatural heteroatom-containing compound such as C−N bond formation among which metal nitrene mediated amination and aziridination have both attracted much attention.[1-3] Nitrogen containing compound are widely used in drug synthesis because nitrogen generally exhibits ability to act as a hydrogen bond donor and/or acceptor which influences the interaction between the medicinal agent and its target significantly.[4] Metal nitrene catalysis reaction can initiate amination to form C−N bond directly.[5-9] Rhodium metal compounds are one of the effective and widely used catalysts to mediate C−H bond amination.[10-13] For the C−N bond formation reaction from rhodium nitrene, concerted insertion via a singlet nitrene and radical recombination via a triplet nitrene are alternative pathways.[14] Du Bois and co-workers have done many researches on dirhodium catalysts and found some of them, including $Rh_2(OAc)_4$ and $Rh_2(esp)_2$, exhibit the catalysis with a concerted but asynchronous mechanism, just like Rh-catalyzed carbene insertion.[15, 16] Our group and co-workers also reported the intramolecular amidation of carbamates prefers the singlet pathway rather than the triplet pathway according to the free energy of activation.[17] And recently we have published further study on dirhodium mediated C−H bond amination mechanism and found the reaction takes place via triplet mecheanism.[18, 19] However, the mechanisms of rhodium-catalyzed amination would be system-dependent and thus detailed explorations on various reactions should be paid attention to.

Recently, Du Bois and co-workers[2, 8, 12, 13, 20-22] designed and synthesized a new catalyst $Rh_2(esp)_2$, a tethered dicarboxylate-derived complex for intramolecular C−H oxidation and this catalyst performed excellent C−H amination with low catalyst loading.[23, 24] The chelating dicarboxylate ligand groups are resistant to ligand exchange and would shroud the dirhodium core even in oxidative conditions.[20] Therefore, the unusual kinetic stability override other dirhodium tetracarboxylate complexes possibly has contributed to the high-efficiency of $Rh_2(esp)_2$.[25] Though the use of $Rh_2(esp)_2$ could

be converse C−H bond into C−N bond via amination effectively, the condensation between the substrate and terminal oxidant is obviously limited for product purifying.[15] The C−H oxidation (sulfamate, carbamate, sulfamide and guanidine, etc.) mediated by rhodium catalysts usually occur under oxidative conditions and require strong electron-withdrawing groups on the nitrene.[5] These limitations are not favored for expanding the scale of potential substrates and the utility of the catalysis reaction. Recently, a new type of reactions with azides has been used for the synthesis of nitrogen heterocycles via intramolecular addition.[26, 27] Reactions with azides involve no oxidants and would release the only byproduct N_2 gas which is environmentally friendly.[28-32] Driver and co-workers have reported the preparation of indoles and carbazoles that involves the catalytic decomposition of aryl azides followed by sp^2 C−H bond amination reactions.[33-38] On the basis of the sp^2 C−H bond amination reactions, Driver and co-workers reported a new type of reactions catalyzed by $Rh_2(esp)_2$ using aryl azides as the N-atom source and it has a high conversion up to 99% (see Scheme 1).[39] These reactions could occur with aryl azides containing *para*-electron-releasing, -neutral, or –withdrawing groups rather than require an electron-withdrawing group on the nitrogen. $Rh_2(esp)_2$ is an unusual dirhodium catalyst that is clear of rapid carboxylate ligand exchange, namely, it exhibits high kinetic stability in reaction solution.[25] In the metal catalyzed C−N bond formation with aryl azides, N_2 gas will be firstly released to form metal nitrene complex which undergoes subsequent nitrene transfer/insertion reaction.[40-42] According to the related experiments, the diastereoisomers of products (dr 50:50) and intramolecular kinetic isotope effect (KIE) of 6.7 corroborate a stepwise C−H bond amination and the rate-determining step is the extrusion of N_2.[39] Therefore, it is necessary to further analyze and understand $Rh_2(esp)_2$ mediated C−H bond amination reactions. In this paper, we report a density functional theory (DFT) computational study of the mechanisms of this dirhodium catalyzed intramolecular aliphatic C−H bond amination of aryl azides. Also, the catalysis nature

differences or similarities between $Rh_2(esp)_2$ (**I** in Figure 1) and other dirhodium catalysts with bridging tetracarboxylate ligand groups (Rh_2L_4) will be discussed.

Scheme 1. $Rh_2(esp)_2$-Catalyzed Intramolecular Aliphatic C−H Bond Amination with Aryl Azides*

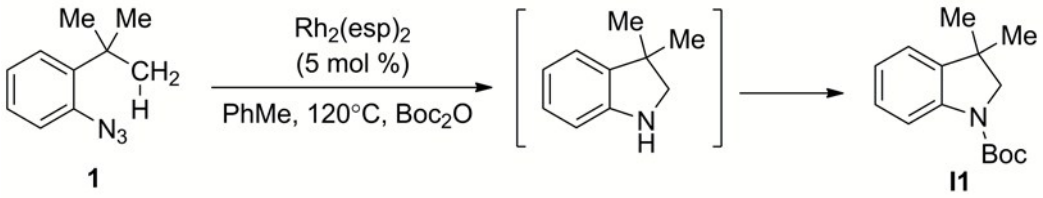

* Yield as isolated after silica gel chromatography: **I1** 84%.[39]

2. Computational Details

Theoretical calculations were performed utilizing Gaussian 09 program.[43] All geometries are fully optimized using DFT method BPW91 with the 6-31G(d) basis sets for C, H, O and N atoms while the 1997 Stuttgart relativistic small-core effective core-potential [Stuttgart RSC 1997 ECP][44, 45] for Rh atoms, augmented with a 4f-function (ζf(Rh) = 1.350),[46] which are donated as BPW91/BS1. BPW91 is a reliable method for metal nitrene mediated reactions, especially in describing the singlet–triplet energy difference (E_{st}) of dirhodium–nitrene complexes.[17-19, 47-49] Intrinsic reaction coordinate (IRC)[50] calculations were done to confirm the reactant and product connecting the corresponding transition states. The energies were calculated at 393.15 K and 1 atm according to the experiment conditions.[39] Natural bond orbital (NBO) analysis[51, 52] and Kohn-Sham frontier orbital analysis were done with the calculated level BPW91/BS1. Solvent effects (in toluene) were estimated using the polarizable continuum model (PCM) with radii and non-electrostatic terms for Truhlar and coworkers' SMD salvation model[53] with a larger basis set 6-311++G(d,p) for C, H, O and N atoms and the same Stuttgart basis sets as BS1 (RSCf) for Rh atoms, which are donated as BS2. Minimum-energy crossing points (MECPs) were located utilizing the MECP program developed by Harvey and co-workers.[54]

In order to obtain accurate thermochemistry predictions and descriptions of weak interaction, we performed geometry optimization and energy calculations of selected important intermediates and transition states at the M06L (the pure functional of Truhlar and Zhao)/BS1 level of theory.[18, 55] Also, the composite basis sets (denoted as BS3) consisting of the basis set 6-311G(d,p) for C, H, O and N atoms and the same Stuttgart basis sets as BS1 for Rh atoms were also employed. These calculations have shown that the BPW91/BS1, M06L/BS1 and BPW91/BS3 optimized geometries are very close, while relative energies can vary by a few kcal/mol with solvent effects at BPW91/BS2 or M06L/BS2 included (see ESI), and they give the same conclusions. Therefore, below, in sake of consistency, we discuss the BPW91/BS1 calculated results unless otherwise specified.

3. Results and Discussions

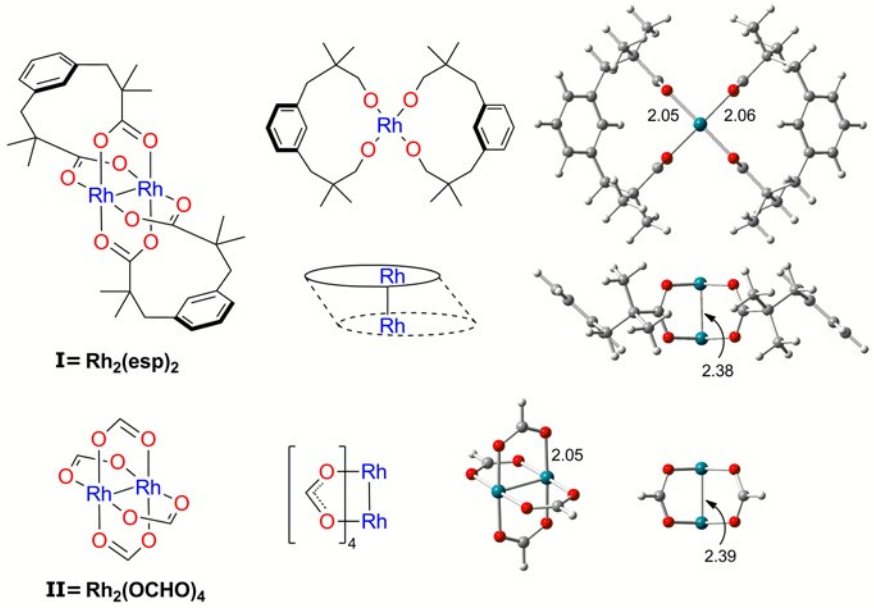

Figure 1. Catalysts in the calculations of the intramolecular C−H bond amination with aryl azides: **I**= $Rh_2(esp)_2$, **II**= $Rh_2(OCHO)_4$.

Based on the survey of catalysts in the related experiments, the reaction yields in the presence of $Rh_2(esp)_2$, $Rh_2(OAc)_4$, $Rh_2(O_2CC_7H_{15})_4$ and $Rh_2(O_2CC_3F_7)_4$ are 75%, 0%, 35% and 20%, respectively.[39] As reported in previous literature, the tetracarboxylate

ligand groups are sensitive to ligand exchange which would inhibit the cycled catalysis of C−H bond amination.[5, 25] However, this ligand exchange event is assumed to be inoperative in order to explore other factors that influence catalytic reactivity and reaction mechanism. To investigate the mechanistic similarities and differences between $Rh_2(esp)_2$ (**I** in Figure 1) and the general dirhodium catalysts with bridging tetracarboxylate ligand (Rh_2L_4), in this paper, a model compound $Rh_2(OCHO)_4$ (**II** in Figure 1) was used to model Rh_2L_4. Figure 1 shows the computed geometries of the catalysts **I** and **II**. Comparing the key bond lengths such as Rh−Rh and Rh−O bond distances in **I** and **II**, they have almost the same values, which indicates these two catalysts have a similar framework and bimetallic interactions.

3.1 Proposed Mechanism of dirhodium Catalyzed C−H Bond Amination with Aryl Azide 1

Scheme 2. Proposed Mechanisms of Rh_2L_n Promoted Intramolecular Aliphatic C−H Bond Amination with Aryl Azide **1**

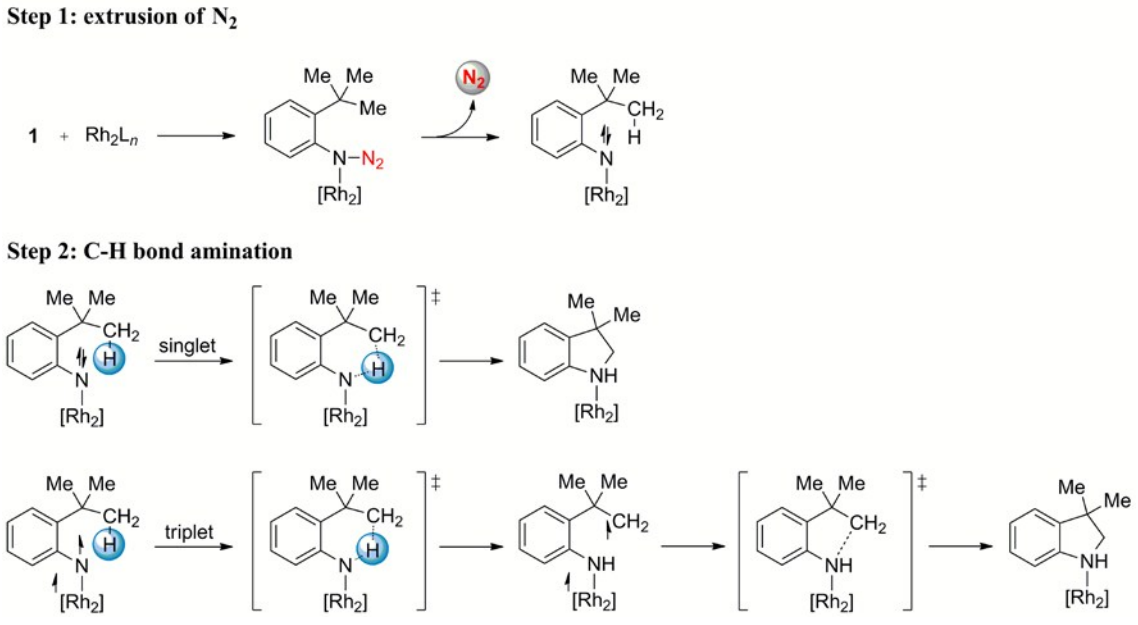

Taking *o-tert*-butylaryl azide **1** in Scheme 1 as a sample substrate, Scheme 2 shows the proposed mechanisms of dirhodium complexes (Rh_2L_n) promoted intramolecular aliphatic C−H bond amination with aryl azides. In Scheme 2, [Rh_2] denotes the

dirhodium paddlewheel catalysts. According to the investigations of related reactions mentioned above, the metal catalyst and the azides combine together via Rh−N bonding before N_2 release.[40] The intramolecular aliphatic C−H bond amination reaction might involve two steps (Scheme 2): i) the first step is extrusion of nitrogen gas from the precursor complex of the metal catalyst and substrate, ii) the second step is conversion of C−H bond into C−N bond, which might take place through singlet or triplet pathway. The concerted singlet pathway could form C−N and N−H bond spontaneously through C−H bond nitrogen insertion while the stepwise triplet pathway would go through H-abstraction followed by diradical recombination or intersystem crossing (ISC).[47] Both the singlet and triplet pathways lead to the final product indolines and the catalyst is regenerated.

Scheme 3. Depicted are labels of the selected atoms in the reaction complexes. O1 and O2 refer to the oxygen atoms coordinated to Rh1 and Rh2 centers, respectively.

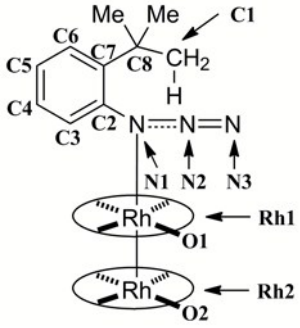

3.2. $Rh_2(esp)_2$ catalyzed amination of aryl azide 1.

As mentioned above, the purpose of this paper is to elucidate the reaction mechanism of dirhodium complex, $Rh_2(esp)_2$ and $Rh_2(tetracarboxylate)_4$ included, catalyzed amination which includes two basic steps: i) extrusion of N_2, ii) nitrene insertion. In this section, the reaction with $Rh_2(esp)_2$ (**I**) as the catalyst is computed and compared with the case for $Rh_2(OCHO)_4$ (**II**). It should be mentioned that the computaional data for $Rh_2(OCHO)_4$ are majorly presented in ESI. For clear descriptions, labels of the atoms in the active sites of reaction complexes are given in Scheme 3.

3.2.1. Metal nitrene formation from $Rh_2(esp)_2$ and aryl azide 1.

As reported in related investigations about metal nitrene catalyzed C−H bond amination with azides, coordination of the metal core could be towards either the α- or γ-nitrogen of the azides.[41, 56] However, the γ-coordination complex may not directly release nitrogen gas but transform into the α- coordination complex which could trigger amination reactions (see Figure S1 in ESI).

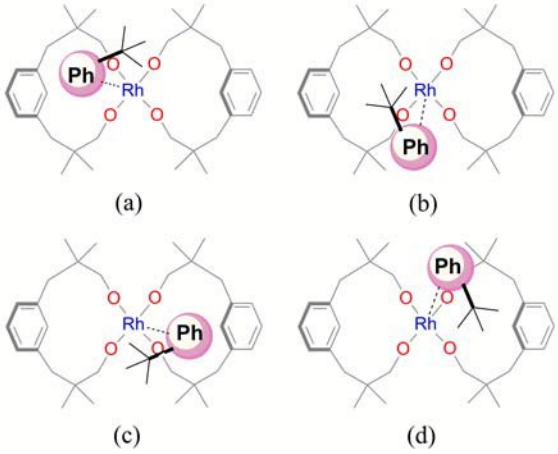

Figure 2. Possible coordination modes of $Rh_2(esp)_2$ and aryl azides.

The two rhodium centers in $Rh_2(esp)_2$ are in equal positions. As shown in Figure 2, the centro-symmetric geometry of $Rh_2(esp)_2$ can provide four positions to recognize and bond with the substrate aryl azide molecule. In order to diminish steric effects, the aryl group and the *tert*-butyl group should be located near two out of the four "caves" divided by the tethered ligands. And from the structure of the catalyst-substrate binding complex in Figure 2a, the aryl azide molecule rotates along Rh−N bond anticlockwise and forms the other three structures (Figures 2b, 2c and 2d). In Figures 2a and 2b, both the aryl group and the *tert*-butyl group are positioned over the less crowded caves. In Figures 2c and 2d, either the aryl group or the *tert*-butyl group is over the crowded cave with a phenyl group pointing inside. On the other hand, the azide moiety (−N=N=N) may be repulsed by the ligand, especially for the structure in Figure 2b.

The four coordination complexes of aryl azide **1** and $Rh_2(esp)_2$ shown in Figure 2 lead to four pathways of metal nitrene formation (see Figure 3). **Ac** has almost the same

energy as **Aa** while **Ab** and **Ad** are 2.3 and 1.7 kcal/mol higher in free energy than **Aa**, respectively. The higher free energies might be mainly ascribed to the steric repulsion between the ligand of **I** and the *tert*-butyl group or the azide moiety of **1**. However, the energy differences are still acceptable and these four isomers could be interchanged with each other. Therefore, only the reaction from **Aa** is discussed in the present paper.

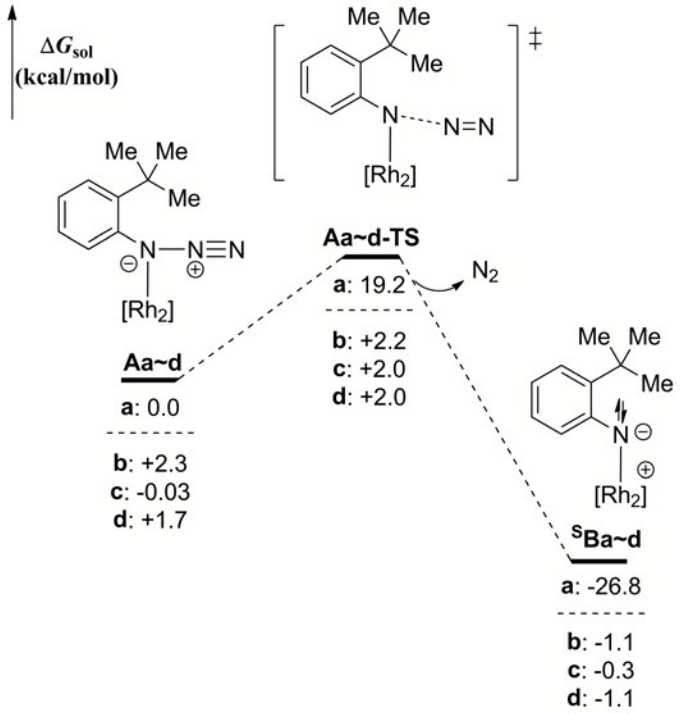

Figure 3. Reaction profiles of metal nitrenoid formation from $Rh_2(esp)_2$ and **1**. The relative Gibbs free energies and thermal energies are presented with **Aa**, **Aa-TS** and **Ba** as the zero points, respectively.

With the coordination between the Rh-atom and *α*-N-atom in **Aa**, the atomic charge on *α*-N-atom decreases which could assist the N_2 loss.[41] The N−N bond cleavage via the transition state **Aa-TS** requires a barrier of 19.2 kcal/mol. The elimination of nitrogen gas is an exothermic process that produces the singlet metal nitrene ^{S}**Ba**. The structures located in the reaction pathway from **Aa** are shown in Figure 4. The coordination of Rh1−N1 (2.31 Å) in the reactant species **Aa** is relatively weak while it obviously becomes stronger in the transition state **Aa-TS** (Rh1−N1, 2.07 Å) with the elongation of N1−N2 bond distance (from 1.26 Å in **Aa** to 1.63 Å in **Aa-TS**). From the NBO charge

analysis, the rhodium centers would help to stabilize the negative-charged nitrogen atom N1 through the reaction process (see Figure 4).

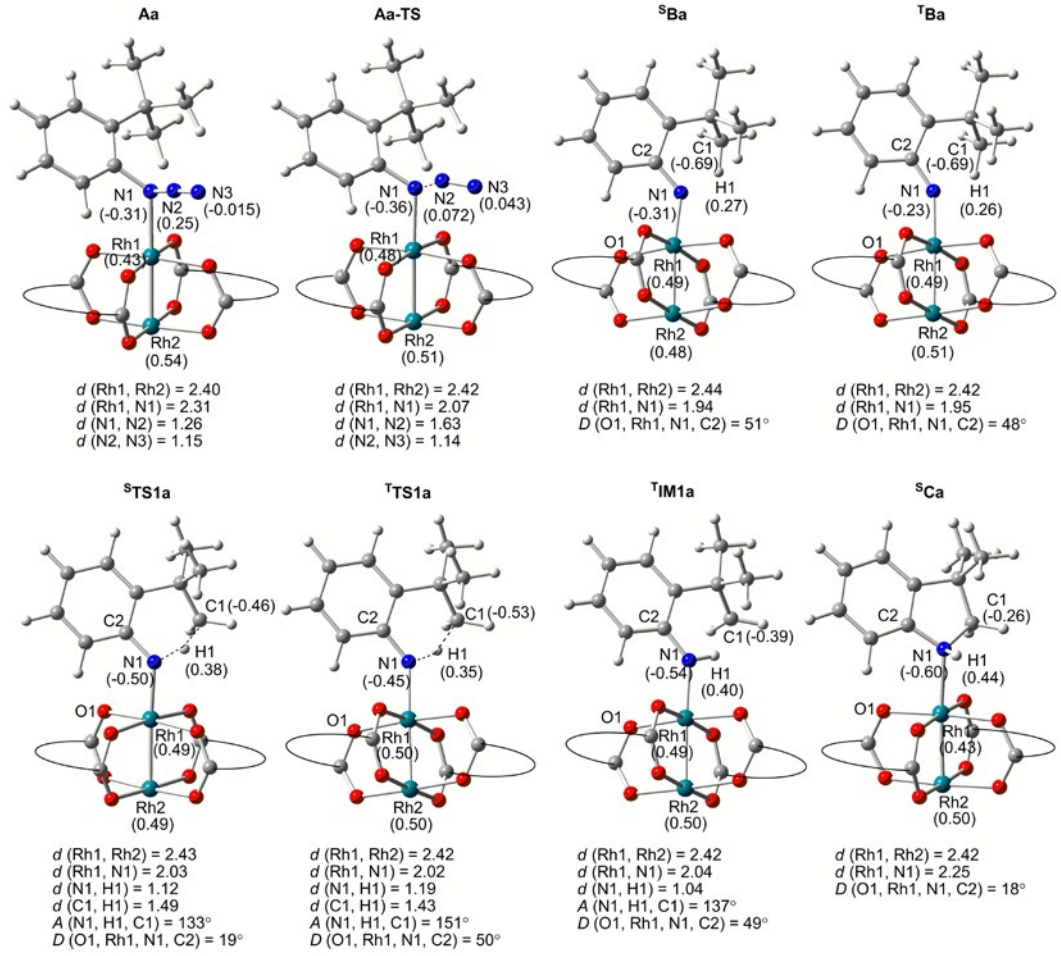

Figure 4. Shown are selected optimized structures in the reaction of $Rh_2(esp)_2$ (**I**) and **1**. The tethered dicarboxylate ligands (esp) are simplified. Selected NBO charges are in parentheses and bond distances are in angstrom.

When comparing the mechanisms of nitrene formation mediated by $Rh_2(esp)_2$ (**I**) and $Rh_2(OCHO)_4$ (**II**) (see ESI), the whole reaction profiles of N_2 extrusion shown in Figures 3 and S1 exhibit identical patterns for the complete reaction pathway. What's more, the geometric parameters in these two reaction systems are comparative in spite of a few differences. For instance, the Rh1−Rh2 bond is slightly longer in the reaction process of $Rh_2(OCHO)_4$ and **1** (Figure S3) than those of $Rh_2(esp)_2$ and **1** (Figure 4), which is probably due to the compacting enhancement from the "esp" ligand in $Rh_2(esp)_2$. From the aspect of energy, the activation energy of **Aa-TS** (19.2 kcal/mol) is

slightly lower than that of **A-TS** (20.0 kcal/mol). This could be ascribed to the weak electron-donating esp ligands.

3.2.2. Metal nitrene mediated amination in Ba.

Following the metal nitrene formation, the resulted active intermediates would undergo subsequent nitrene insertion/C−H bond amination. In consideration of the similar reaction mechanisms for the metal nitrenes **Ba~d** (Figure S5), only the reactions from **Ba** (see Figure 5) and the species on these reaction profiles (Figure 4) will be further discussed.

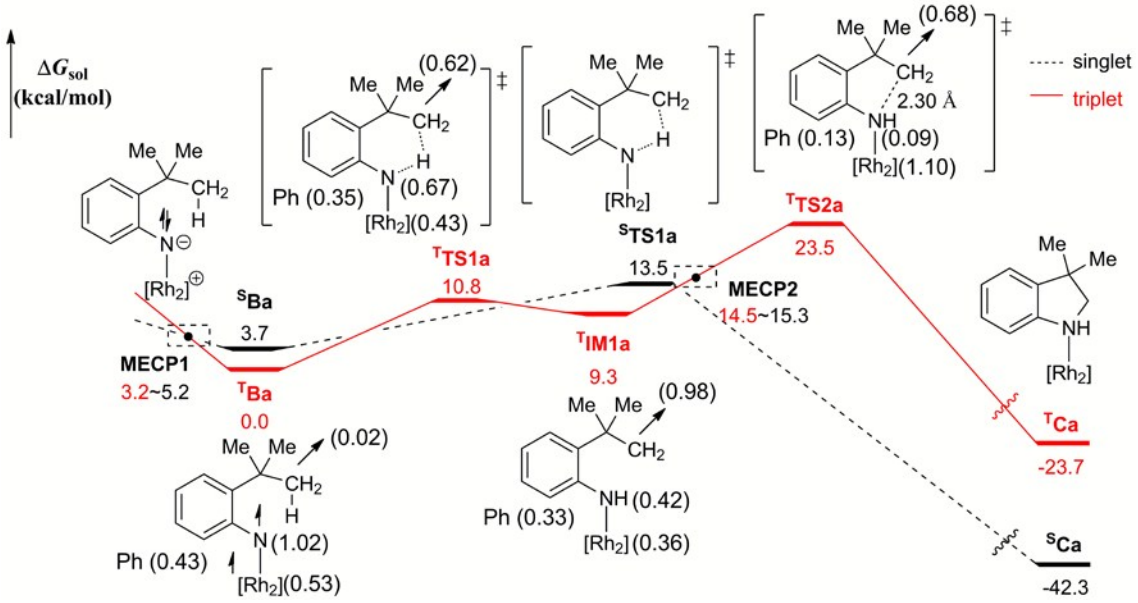

Figure 5. Reaction profiles of C−H bond amination mediated by **Ba**. Spin densities of Rh1-Rh2, N1, C1, Ph(C2~C7) are in parentheses.

As discussed above, the singlet metal nitrene ^{S}**Ba** is formed in the extrusion of N_2 from **Aa** (Figure 3). However, the existence of a minimum energy crossing point (**MECP1**) between the singlet and the triplet profiles allows the formation of the triplet metal nitrene ^{T}**Ba**. At the minimum energy crossing point **MECP1** located before the reactants, the singlet nitrenoid and triplet one are quite close in energy.[56] It should be mentioned that the relative free energies of MECPs are estimated taking the salvation effects into account. Thus, they represent the most possible location areas rather than the accurate crossing points (see Figure S6 in ESI). The triplet metal nitrene ^{T}**Ba** is

more stable than the singlet nitrene ^{S}**Ba** by 3.7 kcal/mol. This is different from the previously reported conclusion obtained from similar reaction systems involving Rh_2L_4 that the ground triplet state of metal nitrene is estimated to be about 2 kcal/mol higher than the singlet state and thus they could coexist with each other.[17] Comparing the structures of the singlet and triplet metal nitrenes, ^{S}**Ba** and ^{T}**Ba**, not only the Rh1−Rh2 and Rh1−N1 bond distances are almost the same, but the dihedral angle *D*(O1, Rh1, N1, C2) is also comparable in ^{T}**Ba** (51˚) with that in ^{S}**Ba** (48˚). On the other hand, the spin densities for Rh1, Rh2, N1 atoms and the phenyl ring (C2~C7) in ^{T}**Ba** are 0.35, 0.18, 1.02 and 0.43, respectively (Figure 5 and Table S2). This means the two unpaired electrons mainly reside on the Rh_2 and N1-Ph(C2~C7) moiety.

For the dirhodium reaction complex, the strong d-p orbital interactions between the $Rh_2^{II,II}$ center and N1 could stabilize the radical species.[19] This would increase the reaction barrier for the H-abstraction process and could possibly further improve the reaction selectivity. This type of metal-metal bonded systems has been extensively discussed in literature and they are suggested to exhibit exceptional efficiency in C−H functionalization rather than mono-metal catalysts. The dirhodium d^{14} electronic configuration were highly effective at metal to ligand π back-bonding and the filled π* orbital of Rh_2L_4 could donate electron-pair,[57] e.g. the π and π(nb) bonding shown in Figure S7. This indicates distinctive metal-metal synergism which endues a metal-metal complex reactivity different from a mono-nuclear metal complex.[58] Furthermore, the unique catalysis is attributed to the three-center/four-electron (3c/4e) bonds in metal-metal bonded intermediates such as carbene and nitrene intermediates Rh−Rh−C(or N) which is suggested to be described as superelectrophilic by virtue of 3c/4e Rh−Rh−C(or N) s and p bonds.[59]

In the singlet pathway of C−H bond amination, the C−H bond cleavage, N−H and C−N bond formation through the transition state ^{S}**TS1a** requires an energy barrier of 13.5 kcal/mol relative to ^{T}**Ba**. For $Rh_2(OCHO)_4$, the barrier is 12.0 kcal/mol relative to ^{T}**B**, respectively (Figure S2 in ESI). The vibration of the unique imaginary frequency

(-659.3 cm^{-1}) in ^{S}**TS1a** shows an evident H-abstraction process accompanied with an initial C−N bond formation. According to the IRC calculation (see Figure S9 in ESI), the concerted singlet pathway exhibits asynchronous characteristic that the hydride-like H1 is transferred prior to the formation of N1−C1 bond. This feature can be seen from the angle *A*(N1,H1,C1) = 133°, and the charge change of H-donor C1(sp^3) from -0.69 for ^{S}**Ba** to -0.46 for ^{S}**TS1a**. However, the weak electron-donating catalyst $Rh_2(esp)_2$ cannot stabilize a potential intermediate followed by H-abstraction step featuring a carbocation and a negative nitrogen center. Therefore, no intermediates or transition states are observed on the way from ^{S}**TS1a** to the final product ^{S}**Ca**. Our previous study has proposed the nature of the singlet pathway is a stepwise process and the fast combination of a carbocation and an electron-sufficient nitrogen center is barrier-free or require an identifiable energy barrier.[18]

In the triplet pathway, two steps are involved: H-abstraction and C−N bond formation. In the H-abstraction step, the activation energy of the transition state ^{T}**TS1a** is 10.8 kcal/mol. For $Rh_2(OCHO)_4$, the barrier is 9.1 kcal/mol relative to ^{T}**B** (Figure S2 in ESI). The spin density for H-donor (C1) increases significantly from 0.02 in ^{T}**Ba** to 0.62 in the triplet transition state ^{T}**TS1a** while the spin density for N1 atom decreases from 1.02 to 0.67. The vibration of the unique imaginary frequency (-1136.1 cm^{-1}) in ^{T}**TS1a** and the IRC calculation for ^{T}**TS1a** (see Figure S10 in ESI) shows this is a complete hydrogen-migration process and no signs of C−N bond formation. This C−H homolytic cleavage mediated by $Rh_2(esp)_2$ results in the intermediate ^{T}**IM1a**. The spin densities for Rh1, Rh2, N1, C1 atoms and the phenyl ring (C2~C7) in ^{T}**IM1a** are 0.24, 0.12, 0.42, 0.98 and 0.33, respectively. It means the two unpaired electrons mainly reside on the C1, Rh_2 core and N1-Ph(C2~C7) moiety. The intermediate ^{T}**IM1a** on the triplet reaction profile is close to the triplet transition state ^{T}**TS1a** in energy. This could be attributed to the relatively small geometry change from the transition state to the corresponding reactive intermediate. The diradical intermediate ^{T}**IM1a** rebound in a subsequent step via the radical coupling transition state ^{T}**TS2a** requiring a high barrier (from ^{T}**Ba** to

^{T}**TS2a**, 23.5 kcal/mol; from ^{T}**IM1a** to ^{T}**TS2a**, 14.2 kcal/mol). For $Rh_2(OCHO)_4$, the barrier of the radical coupling is 23.4 kcal/mol relative to ^{T}**B** and 15.4 kcal/mol relative to ^{T}**IM1** (Figure S2 in ESI). As we previously reported, this type of diradical recombination step requires an identifiable energy barrier (~15 kcal/mol).[18] However, this radical recombination may not be observed, because there exists a spin crossing via **MECP2** between the triplet and singlet energy profiles. After spin crossover to the singlet pathway, the final product ^{S}**Ca** is reached. Therefore, the overall energy barrier of the triplet pathway is determined by the relative energy of **MECP2**. It should be mentioned that our previous studies on the reactions of dirhodium tetracarboxylate (Rh_2(formate)$_4$ and $Rh_2(OAc)_4$) catalyzed nitrene insertion into C–H bonds generally suggest the closed-shell singlet transition state is lower in energy than the open-shell triplet transition state in the H-abstraction step.[17-19] Also, we have done calculations of MECPs in amination reactions catalyzed by dirhodium tetracarboxylate and basically MECP is located on the way from the triplet reactant complex to the triplet H-abstraction transition state which suggests a spin crossover to the closed-shell singlet energy profile.[18, 19]

In order to understand the triplet pathway in depth, the mulliken spin distribution along the reaction coordinate for the triplet states is presented in Figure 6. In the H-abstraction step, the spin density on the Rh_2 center in the triplet reactant complex ^{T}**Ba** is significantly less than 1.0. With the spin on N1, Rh_2, Ph moieties partially transferred to C1 via ^{T}**TS1a**, the spin densities on the Rh_2 center decreases further in ^{T}**IM1a**. In the subsequent C−N bond formation step, the spin density on the Rh_2 center increases to larger than 1.0 in ^{T}**TS2a** and the triplet product complex ^{T}**Ca** holds the major spin density on the Rh_2 center. As we previously reported, the $Rh_2^{II,II}$ dimer in ^{T}**TS2a** would be oxidized to a mixed-valent $Rh_2^{II,III}$ dimer and a NR radical.[19] This spin-orbital coupling in the Rh_2 center forming C−N bond is an energy-consuming process.[18]

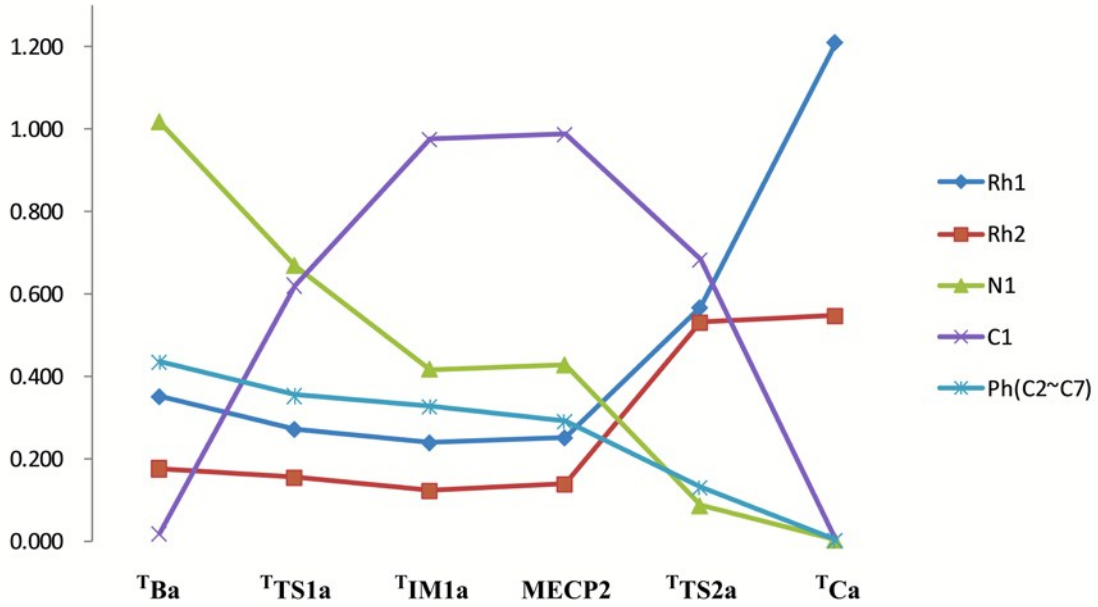

Figure 6. Mulliken spin distribution along the reaction coordinate for the triplet states in reaction of $Rh_2(esp)_2$ and **1**.

From the metal nitrenes $^{S/T}$**Ba** to the transition states $^{S/T}$**TS1a**, the Rh1−N1 bond elongates slightly and the charge of N1 atom becomes more negative (see Figure 4). It is worth noting that the dihedral angle *D*(O1, Rh1, N1, C2) is much smaller in ^{S}**TS1a** (19˚) than that in ^{S}**Ba** (51˚) but the values in ^{T}**TS1a** (50˚) and ^{T}**Ba** (48˚) are identical. Comparing the singlet and triplet transition states, ^{S}**TS1a** and ^{T}**TS1a**, the distance of N1-H1 in ^{T}**TS1a** is longer and C1−H1 shorter. As seen in the geometry of the final product-catalyst complex ^{S}**Ca**, the distance of Rh1−N1 elongates to 2.25 Å which is close to that in **Aa** (2.31 Å); and Rh1 charge reduces to 0.43 which equals that in **Aa**.

It should be mentioned that the unstable triplet intermediate ^{T}**IM1a** would possibly go through two alternative C−N formation pathways. One is direct recombination of diradical via ^{T}**TS2a** which is discussed above. Another pathway is a N−H swing/diradical recombination process (see Figure S8 in ESI). Calculations show that these two pathways in the triplet mechanisms are competitive. Therefore, the N−H swing process could possibly lead to racemic products.[18]

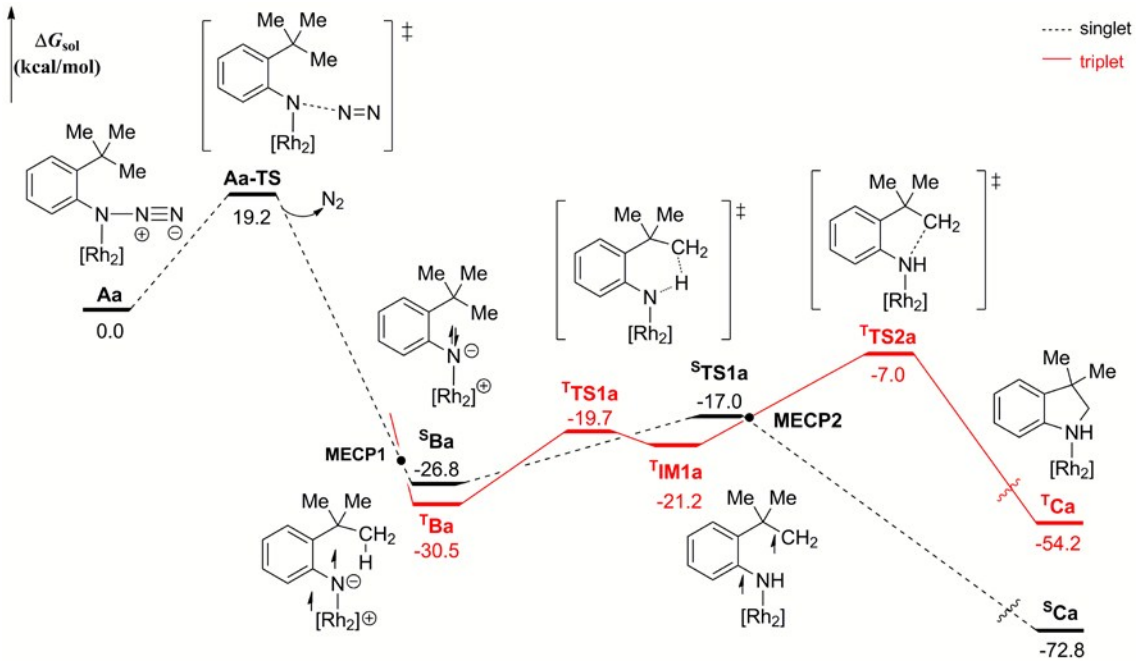

Figure 7. Reaction profiles of $Rh_2(esp)_2$ catalyzed amination of C−H bond.

3.3. Key Mechanistic Features of Dirhodium Catalyzed C−H Bond Amination with Aryl Azides.

From results above, $Rh_2(esp)_2$ and $Rh_2(OCHO)_4$ (see ESI) catalyzed C−H amination majorly share an identical mechanism, including the PES pattern and the structure features of the reactants, transition states and products. The whole PES for the $Rh_2(esp)_2$ case is shown in Figure 7. The tethered ligands esp of $Rh_2(esp)_2$ would not obviously affect the amination reaction mechanism. Based on the experimental observations,[39] esp ligand can prevent oxidation in the reaction solution and protect the geometry of the dirhodium complex which increases the conversion of the catalytic reaction cycle. On the other hand, reactions with mononuclear catalysts known to catalyze N-atom-transfer reactions, such as $[Rh(cod)_2]SO_3CF_3$, $[Rh(PPh_3)_3]Cl$ and $[Rh(cod)OMe]_2$ (cod =1,5-cyclooctadiene), are unsuccessful in producing indoline product.[39] And as we discussed above, the strong d-p orbital interactions between the $Rh_2^{II,II}$ center and nitrene N could stabilize the radical species and could possibly further enhance the

reaction selectivity. Therefore, the combination of $Rh_2^{II,II}$ dimer and ligands as "security guard" is the key to success of the aliphatic C−H amination involved in this paper.

4. Conclusions

In conclusion, dirhodium catalysts Rh_2L_n, such as $Rh_2(esp)_2$ and $Rh_2(OCHO)_4$, mediated aliphatic C−H bond amination of aryl azides show a general mechanism. Firstly, the dirhodium complex coordinates with the substrate leading to the extrusion of nitrogen gas to produce metal nitrene. This is the rate-determining step and significantly exothermic. A minimum energy crossing point is located in this step and leads to the singlet metal nitrene or the triplet metal nitrene. Secondly, the dirhodium metal nitrene forms C−N bond via intramolecular nitrene insertion to C−H bond through two possible reaction pathways. One is the singlet concerted asynchronous pathway which results in direct insertion of metal nitrene into C−H bond. Another one is the triplet stepwise pathway in which hydrogen atom transfer followed by diradical combination. However, calculations show the diradical recombination requires a relatively high barrier more than 20 kcal/mol. There is a minimum energy crossing point located between the singlet and triplet pathways which leads the reaction towards the singlet pathway. The tethered ligands joined to the rhodium centers of $Rh_2(esp)_2$ give aid to stabilize the substrate-catalyst complex and play a role as "security guard" to protect the dirhodium core, but they do not indicate significant influence on the reaction mechanisms of metal nitrene catalyzed amination of aliphatic C−H bond of aryl azides.

Acknowledgements

The authors gratefully acknowledge the National Natural Science Foundation of China (Grant Nos. 21173273, 21203256, 21373277, 21473261, 21573292) and the Guangdong Provincial Natural Science Foundation (Nos. 2015A030313185, 2015A030306027). This work was partially sponsored by the high-performance grid computing platform of

Sun Yat-sen University and supported in part by the Guangdong Province Key Laboratory of Computational Science and the Guangdong Province Computational Science Innovative Research Team.

References

1 H. M. L. Davies and J. R. Manning, *Nature*, 2008, **451**, 417-424.

2 H. D. Davies, H. M. L., J. Du Bois and J. Q. Yu, *Chem. Soc. Rev.*, 2011, **40**, 1855-1856.

3 H. J. Lu, H. L. Jiang, Y. Hu, L. Wojtas and X. P. Zhang, *Chem. Sci.*, 2011, **2**, 2361-2366.

4 F. Collet, R. H. Dodd and P. Dauban, *Chem. Commun.*, 2009, 5061-5074.

5 J. Du Bois, *Org Process Res. Dev.*, 2011, **15**, 758-762.

6 H. Lebel, C. Trudel and C. Spitz, *Chem. Commun.*, 2012, **48**, 7799-7801.

7 T. W. Lyons and M. S. Sanford, *Che. Rev.*, 2010, **110**, 1147-1169.

8 M. E. Harvey, D. G. Musaev and J. Du Bois, *J. Am. Chem. Soc.*, 2011, **133**, 17207-17216.

9 E. R. King, E. T. Hennessy and T. A. Betley, *J. Am. Chem. Soc.*, 2011, **133**, 4917-4923.

10 J. Ryu, K. Shin, S. H. Park, J. Y. Kim and S. Chang, *Angew. Chem., Int. Ed.*, 2012, **51**, 9904-9908.

11 A. Nörder, S. A. Warren, E. Herdtweck, S. M. Huber and T. Bach, *J. Am. Chem. Soc.*, 2012, **134**, 13524-13531.

12 J. Du Bois, K. W. Fiori, C. G. Espino and B. H. Brodsky, *Tetrahedron*, 2009, **65**, 3042-3051.

13 J. Du Bois and D. N. Zalatan, *J. Am. Chem. Soc.*, 2008, **130**, 9220-9221.

14 Q. Zhang, C. Wu, L. Zhou and J. Li, *Organometallics*, 2013, **32**, 415-426.

15 K. W. Fiori, C. G. Espino, B. H. Brodsky and J. Du Bois, *Tetrahedron*, 2009, **65**, 3042-3051.

16 E. Nakamura, N. Yoshikai and M. Yamanaka, *J. Am. Chem. Soc.*, 2002, **124**, 7181-7192.

17 X. Lin, C. Zhao, C.-M. Che, Z. Ke and D. L. Phillips, *Chem. – Asian J.*, 2007, **2**, 1101-1108.

18 X. Zhang, H. Xu and C. Zhao, *J. Org. Chem.*, 2014, **79**, 9799-9811.

19 X. Zhang, Z. Ke, N. J. DeYonker, H. Xu, Z.-F. Li, X. Xu, X. Zhang, C.-Y. Su, D. L. Phillips and C. Zhao, *J. Org. Chem.*, 2013, **78**, 12460-12468.

20 J. L. Roizen, M. E. Harvey and J. Du Bois, *Acc. Chem. Res.*, 2012, **45**, 911-922.

21 C. G. Espino and J. Du Bois, *Abstr. Pap. Am. Chem. S.*, 2003, **226**, U238-U238.

22 J. Du Bois and C. G. Espino, *Angew. Chem. Int. Ed.*, 2001, **40**, 598-600.

23 J. Du Bois, C. G. Espino, K. W. Fiori and M. Kim, *J. Am. Chem. Soc.*, 2004, **126**, 15378-15379.

24 J. Du Bois, T. Kurokawa and M. Kim, *Angew. Chem. Int. Ed.*, 2009, **48**, 2777-2779.

25 J. Du Bois and D. N. Zalatan, *J. Am. Chem. Soc.*, 2009, **131**, 7558-7559.

26 B. C. G. Soderberg, *Curr. Org. Chem.*, 2000, **4**, 727-764.

27 G. Hajos and Z. Riedl, *Curr. Org. Chem.*, 2009, **13**, 791-809.

28 T. G. Driver, *Org. Biomol. Chem.*, 2010, **8**, 3831-3846.

29 T. Katsuki, *Chem. Lett.*, 2005, **34**, 1304-1309.

30 S. Bräse, C. Gil, K. Knepper and V. Zimmermann, *Angew. Chem. Int. Ed.*, 2005, **44**, 5188-5240.

31 H. Lu, J. Tao, J. E. Jones, L. Wojtas and X. P. Zhang, *Org. Lett.*, 2010, **12**, 1248-1251.

32 V. Subbarayan, J. V. Ruppel, S. Zhu, J. A. Perman and X. P. Zhang, *Chem. Commun.*, 2009, 4266-4268.

33 B. J. Stokes, K. J. Richert and T. G. Driver, *J. Org. Chem.*, 2009, **74**, 6442-6451.

34 B. J. Stokes, B. Jovanović, H. Dong, K. J. Richert, R. D. Riell and T. G. Driver, *J. Org. Chem.*, 2009, **74**, 3225-3228.

35 M. Shen, B. E. Leslie and T. G. Driver, *Angew. Chem.*, 2008, **120**, 5134-5137.

36 H. Dong, R. T. Latka and T. G. Driver, *Org. Lett.*, 2011, **13**, 2726-2729.

37 H. Dong, M. Shen, J. E. Redford, B. J. Stokes, A. L. Pumphrey and T. G. Driver, *Org. Lett.*, 2007, **9**, 5191-5194.

38 B. J. Stokes, H. Dong, B. E. Leslie, A. L. Pumphrey and T. G. Driver, *J. Am. Chem. Soc.*, 2007, **129**, 7500-7501.

39 Q. Nguyen, K. Sun and T. G. Driver, *J. Am. Chem. Soc.*, 2012, **134**, 7262-7265.

40 V. Lyaskovskyy, A. I. O. Suarez, H. Lu, H. Jiang, X. P. Zhang and B. de Bruin, *J. Am. Chem. Soc.*, 2011, **133**, 12264-12273.

41 A. I. Olivos Suarez, H. Jiang, X. P. Zhang and B. de Bruin, *Dalton Trans.*, 2011, **40**, 5697-5705.

42 W. G. Shou, J. Li, T. Guo, Z. Lin and G. Jia, *Organometallics*, 2009, **28**, 6847-6854.

43 M. J. T. Frisch, G. W.; Schlegel, H. B.; Scuseria, G. E.; Robb, M. A.; Cheeseman, J. R.; Scalmani, G.; Barone, V.; Mennucci, B.; Petersson, G. A.; Nakatsuji, H.; Caricato, M.; Li, X.; Hratchian, H. P.; Izmaylov, A. F.; Bloino, J.; Zheng, G.; Sonnenberg, J. L.; Hada, M.; Ehara, M.; Toyota, K.; Fukuda, R.; Hasegawa, J.; Ishida, M.; Nakajima, T.; Honda, Y.; Kitao, O.; Nakai, H.; Vreven, T.; Montgomery, J. A., Jr.; Peralta, J. E.; Ogliaro, F.; Bearpark, M.; Heyd, J. J.; Brothers, E.; Kudin, K. N.; Staroverov, V. N.; Kobayashi, R.; Normand, J.; Raghavachari, K.; Rendell, A.; Burant, J. C.; Iyengar, S. S.; Tomasi, J.; Cossi, M.; Rega, N.; Millam, J. M.; Klene, M.; Knox, J. E.; Cross, J. B.; Bakken, V.; Adamo, C.; Jaramillo, J.; Gomperts, R.; Stratmann, R. E.; Yazyev, O.; Austin, A. J.; Cammi, R.; Pomelli, C.; Ochterski, J. W.; Martin, R. L.; Morokuma, K.; Zakrzewski, V. G.; Voth, G. A.; Salvador, P.; Dannenberg, J. J.; Dapprich, S.; Daniels, A. D.; Farkas, Ö.; Foresman, J. B.; Ortiz, J. V.; Cioslowski, J.; Fox, D. J. Gaussian 09, revision A.01; Gaussian, Inc.: Wallingford, CT, 2009.

44 A. Henglein, *J. Phys. Chem.*, 1993, **97**, 5457-5471.

45 U. Steinbrenner, A. Bergner, M. Dolg and H. Stoll, *Mol. Phys.*, 1994, **82**, 3-11.

46 W. H. Lam, K. C. Lam, Z. Lin, S. Shimada, R. N. Perutz and T. B. Marder, *Dalton Trans.*, 2004, 1556-1562.

47 R. Lorpitthaya, Z.-Z. Xie, K. B. Sophy, J.-L. Kuo and X.-W. Liu, *Chem. – Eur. J.*, 2010, **16**, 588-594.

48 R. Lorpitthaya, Z. Z. Xie, J. L. Kuo and X. W. Liu, *Chem. – Eur. J.*, 2008, **14**, 1561-1570.

49 X. F. Lin, J. A. Sun, Y. Y. Xi and B. Pang, *Comput. Theor. Chem.*, 2011, **963**, 284-289.

50 J. B. Foresman, T. A. Keith, K. B. Wiberg, J. Snoonian and M. J. Frisch, *J. Phys. Chem.*, 1996, **100**, 16098-16104.

51 A. E. Reed, L. A. Curtiss and F. Weinhold, *Chem. Rev.*, 1988, **88**, 899-926.

52 A. E. Reed, R. B. Weinstock and F. Weinhold, *J. Chem. Phys.*, 1985, **83**, 735-746.

53 A. V. Marenich, C. J. Cramer and D. G. Truhlar, *J. Phys. Chem. B*, 2009, **113**, 6378-6396.

54 J.N. Harvey, M.Aschi, H. Schwarz and W. Koch, *Theor. Chem. Accts.*, 1998, **99**, 95.

55 Y. Zhao and D. G. Truhlar, *J. Chem. Phys.*, 2006, **125**, 194101-194118.

56 R. Waterman and G. L. Hillhouse, *J. Am. Chem. Soc.*, 2008, **130**, 12628-12629.

57 R. S. Drago, S. P. Tanner, R. M. Richman and J. R. Long, *J. Am. Chem. Soc.*, 1979, **101**, 2897-2903.

58 R. S. Drago, J. R. Long and R. Cosmano, *Inorg. Chem.*, 1981, **20**, 2920-2927.

59 J. F. Berry, *Dalton Trans.*, 2012, **41**, 700-713.

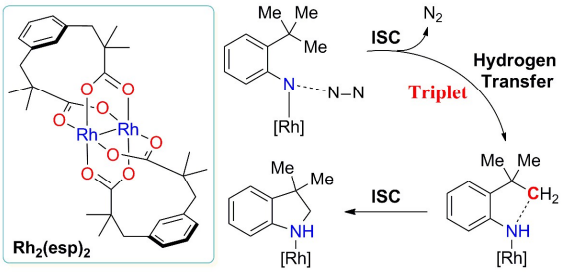

An in-depth DFT study on the dirhodium-catalyzed intramolecular aliphatic C−H bond amination of aryl azides considering ISC.